Langmuir

Article

pubs.acs.org/Langmuir

Formation of Self-Assembled Monolayers of π-Conjugated Molecules on TiO_2 Surfaces by Thermal Grafting of Aryl and Benzyl Halides

Caroline R. English, Lee M. Bishop, Jixin Chen, and Robert J. Hamers*

Department of Chemistry, University of Wisconsin-Madison, 1101 University Avenue, Madison, Wisconsin 53706, United States

Supporting Information

ABSTRACT: We demonstrate the formation of molecular monolayers of π-conjugated organic molecules on nanocrystalline TiO_2 surfaces through the thermal grafting of benzyl and aryl halides. X-ray photoelectron spectroscopy and Fourier-transform infrared spectroscopy were used to characterize the reactivity of aryl and benzyl chlorides, bromides, and iodides with TiO_2 surfaces, along with controls consisting of nonhalogenated compounds. Our results show that benzyl and aryl halides follow a similar reactivity trend (I > Br > Cl ≫ H). While the ability to graft benzyl halides is consistent with the well-known Williamson ether synthesis, the grafting of aryl halides has no similar precedent. The unique reactivity of the TiO_2 surface is demonstrated using nuclear magnetic resonance spectroscopy to compare the surface reactions with the liquid-phase interactions of benzyl and aryl iodides with *tert*-butanol and -butoxide anion. While the aryl iodides show no detectable reactivity with a *tert*-butanol/*tert*-butoxide mixture, they react with TiO_2 within 2 h at 50 °C. Atomic force microscopy studies show that grafting of 4-iodo-1-(trifluoromethyl)benzene onto the rutile TiO_2(110) surface leads to a very uniform, homogeneous molecular layer with a thickness of ∼0.45 nm, demonstrating formation of a self-terminating molecular monolayer. Thermal grafting of aryl iodides provides a facile route to link π-conjugated molecules to TiO_2 surfaces with the shortest possible linkage between the conjugated electron system and the TiO_2.

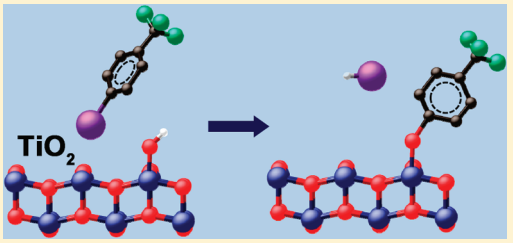

INTRODUCTION

The integration of π-conjugated molecules with metal oxide surfaces provides a way to combine the tunable electronic and chemical properties of organic molecules with the mechanical and electronic properties of inorganic semiconductors, as demonstrated by recent advances in dye-sensitized solar cells.[2−4] The overall properties of such hybrid systems are often dominated by the interfacial chemistry that connects the organic molecules with the inorganic substrates. While a number of different molecule-to-surface linkages have been investigated,[5,6] most research on TiO_2 makes use of simple carboxylate linkages, linking the molecular systems to the surface via the electrostatic binding between the carboxylate groups and the exposed, coordinatively unsaturated Ti^{4+} atoms present at the surface.[7−9] Other approaches to functionalization of TiO_2 have included use of silanes,[10−16] phosphonic acids, and phosphonates,[16−20] formation of ether linkages from alcohols,[21] and photochemical grafting of alkenes.[22,23] The desire to improve the overall stability and electron-transfer properties of molecules at surfaces leads to continued interest in the development of new approaches for linking π-conjugated molecules to TiO_2 and other inorganic semiconductors.

Surfaces of TiO_2 in both anatase and rutile phases expose Ti and O atoms having coordination numbers N lower than the bulk values of $N = 6$ for Ti and $N = 3$ for oxygen. Under ambient conditions, water dissociates on the surface, with the H^+ ions protonating exposed O atoms and OH^- groups bonding to exposed Ti ions. TiO_2 surfaces have at least two distinct types of −OH groups, referred to as "terminal" and "bridging" hydroxyl groups, as depicted in Figure 1.[24,25] The former arises from −OH groups binding to undercoordinated

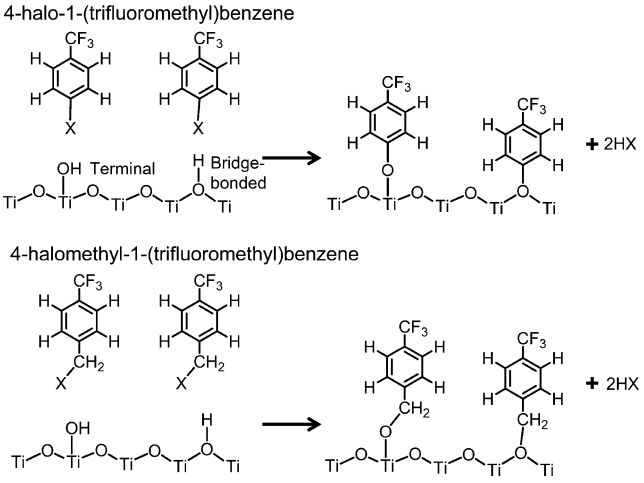

Figure 1. Reaction of aryl halides (top) and benzyl halides (bottom) with hydroxyl groups on the TiO_2 surface. Both terminal and bridge-bonded hydroxyl groups[1] are shown.

Received: January 18, 2012
Revised: March 14, 2012
Published: March 26, 2012

Ti ions, while the latter arises from H^+ binding to surface oxygen atoms that are bound to two Ti ions (instead of 3 as in the bulk). The net result is a surface partially covered with −OH groups. The number, type, and protonation state of the hydroxyl groups can be further manipulated through processes such as exposure to acidic or basic conditions or by heat treatments. Under ambient conditions on microcrystalline samples, the density is typically 3−4 −OH groups/nm^2,[26,27] covering roughly 20−40% of the available surface sites.

Instead of using electrostatic bonding of carboxylate groups to the surface Ti ions, an alternative approach to binding molecules to TiO_2 surfaces under benchtop (nonvacuum) conditions is to develop new surface linkages based on the chemistry of the surface hydroxyl groups.[28,29] Previous work showed that exposing TiO_2 samples in vacuum to ethyl iodide vapor followed by heating to >100 °C yielded surface ethoxy groups, and subsequent work showed that exposing TiO_2 to iodobenzene vapor in vacuum followed by heating to >150 °C for 2 h produced surface phenoxy groups.[30] Recently, we showed[29] that liquid alkyl iodides form monolayers on hydroxylated TiO_2 surfaces under near-ambient conditions (mild heating), as a convenient route to functionalized TiO_2 surfaces via simple benchtop chemistry.

The interaction of organic halides with surface hydroxyl groups appears formally equivalent to the well-known Williamson ether synthesis of organic chemistry.[31] In the Williamson ether synthesis, an organic alcohol R−OH (usually deprotonated to form the alkoxides, $R-O^-$) reacts with an alkyl halide R′−X to form the ether linkage while eliminating HX:

$$R-OH + R'-X \rightarrow R-O-R' + HX$$

The Williamson ether synthesis readily takes place with benzyl and primary alkyl halides via a bimolecular nucleophilic substitution (S_N2) mechanism.[32] While this reaction is facile at the sp^3-hybridized carbon atoms of benzyl and primary alkyl halides, similar etherification reactions with aromatic halides such as aryl halides (in which a halide is directly bonded to a benzene ring) are much less effective and typically proceed by nucleophilic aromatic substitution or radical reaction mechanisms, if they proceed at all.[32−36] Despite these difficulties, the possibility of using aromatic halides as a pathway to molecular layers on surfaces such as TiO_2 is of significant interest because the resulting structure would have a direct linkage between the O atoms of a (hydroxylated) TiO_2 surface and a C atom whose electrons are part of the π-conjugated electron system of the molecule. Figure 1 illustrates the binding configurations on a TiO_2 surface that would result from surface hydroxyl groups reacting with aryl halides and benzyl halides.

Here, we report an investigation of the interactions of aryl and benzyl halides with TiO_2 surfaces using X-ray photoelectron spectroscopy (XPS), Fourier-transform infrared (FTIR) spectroscopy, and atomic force microscopy (AFM). We use the compounds 4-halo-1-(trifluoromethyl)benzene and 4-halomethyl-1-(trifluoromethyl)benzene, depicted in Figure 1, as model systems. Our results show that aryl and benzyl iodides will readily graft to TiO_2 with cleavage of the C−I bond with only mild heating, leading to phenyl-terminated molecular layers. AFM images of the sample reacted with the aryl iodide show formation of smooth, homogeneous molecular layers. Some reactivity is also observed for the bromo-compounds, while the chloro-compounds show little or no reactivity. The results demonstrate the ability to form well-defined molecular layers in which π conjugation extends directly to the molecule-surface bond. Because interfacial charge transfer is largely controlled by the degree of overlap of the wave functions of the molecule and substrate,[9,37,38] this approach may provide a convenient route to improved TiO_2−molecule interfaces with facile charge-transfer properties.

EXPERIMENTAL SECTION

Preparation of TiO_2 Nanocrystalline Thin Films. Nanocrystalline TiO_2 films were made using a commercially available paste (Ti-Nanoxide T20/SP, Solaronix, Switzerland) containing 20 nm diameter anatase TiO_2 nanoparticles. The TiO_2 paste was screen-printed onto substrates consisting of single-crystal Si(001) wafers with a thin evaporated Ti film to provide good adhesion to the TiO_2. Substrates used for XPS experiments used a Ti film 100 nm thick on low-resistivity (<0.1 Ω cm) wafers to provide good electrical conductivity. For infrared studies, we used high-resistivity, float-zone-refined Si(001) wafer and a thinner (20 nm) Ti film; the thin Ti film provides good adhesion of the nanoparticle film to the Si substrate while also reducing optical interference effects that otherwise arise from reflections at the TiO_2−Ti interface. On all samples, the TiO_2 film was prepared by screen-printing. The resulting nanoparticle film was immediately dried at 110 °C and then annealed by gradually heating to 500 °C over 30 min, followed by an additional 15 min at 500 °C. Immediately before use, the TiO_2 nanoparticle films received either an acid-piranha treatment (Caution! Piranha solution is extremely dangerous, and proper safety precautions must be followed) or a NaOH (pH = 11) treatment for 20−30 min. The piranha solution consisted of a mixture of 98% concentrated H_2SO_4 and 30% hydrogen peroxide in a 3:1 volumetric ratio. Samples were then rinsed a minimum of three times with isopropanol and dried with N_2 after each rinse.

Preparation of Single-Crystal TiO_2 Samples. Single-crystal rutile TiO_2 (110) (Crystek) samples were ultrasonically agitated in methanol for 10 min and then placed below a low-pressure Hg lamp in air for 30 min; 185 nm light from the lamp generates a small amount of ozone that removes traces of organic contamination. Afterward, the samples received an HF etch (48 wt % in water) for 30 min before being annealed for 2 h at 900 °C. Directly before use, samples received either an acid-piranha treatment or a base (pH = 11) treatment for 20−30 min. Samples were then rinsed a minimum of three times with isopropanol and dried with N_2 after each rinse.

Thermal Grafting of Halogenated Organic Compounds to TiO_2 Surface. Grafting reactions were performed by immersing TiO_2 samples into neat organic compound and heating in an oven; exposure to light was minimized to avoid photochemical reactions. All grafting compounds were used as received from Sigma-Aldrich except for iodomethyl-TFMB, which is not commercially available and was therefore synthesized and purified as described in the Supporting Information. A range of reaction times was explored; unless otherwise specified, data reported here used a reaction time of 24 h. Grafting experiments were conducted at a temperature of 50 °C for all reactions except those involving iodomethyl-TFMB. Because the melting point of this compound is higher than 50 °C, all reactions using it were conducted at 80 °C. Upon reaction completion, all samples were rinsed a minimum of three times with isopropanol and dried with N_2 after each rinse.

Reactivity of Iodo Compounds toward *tert*-Butanol. Reactions of 1-(iodomethyl)-4-(trifluoromethyl)benzene and 1-iodo-4-(trifluoromethyl)benzene with *tert*-butanol were performed under the same reaction conditions as those used for the TiO_2 samples. *tert*-Butanol was chosen because its tertiary structure mimics the geometry of TiO_2 surface hydroxyl groups. In some experiments, sodium *tert*-butoxide (Aldrich, 97%) was used to explore the reactivity of the deprotonated alcohol. Reaction progress was monitored by NMR spectroscopic analysis.

X-ray Photoelectron Spectroscopy. X-ray photoelectron spectroscopy (XPS) was performed using a custom-built XPS system (Physical Electronics Inc., Eden Prairie, MN) consisting of a model 10-610 K_α X-ray source (1486.6 eV photon energy) with a model 10-420

dx.doi.org/10.1021/la300271h | *Langmuir* 2012, 28, 6866−6876

toroidal monochromator and a model 10-360 hemispherical analyzer with a 16-channel detector array; electrons were typically collected at an emission angle of 45° from the surface normal. The analyzer was typically operated with a 58.7 eV pass energy that yielded an analyzer energy resolution of 0.88 eV. Procedures for analyzing XPS data and converting to coverages are described in the Supporting Information.

Fourier-Transform Infrared (FTIR) Spectroscopy. Infrared spectroscopy was performed using a Bruker Vertex 70 FTIR spectrometer with a Veemax II variable-angle single-bounce reflection accessory. A liquid nitrogen cooled HgCdTe detector was used. Measurements were made with a resolution of 4 cm^{-1} at a 50° angle of incidence from the surface normal using p-polarized light. Reference (background) samples consisted of Si samples with an evaporated 20 nm Ti film that received the same heat treatment as the actual samples. Absorbance spectra were measured before and after reaction and then subtracted to eliminate absorption features of the TiO_2 film itself and bring out the changes induced by the surface reactions. In some cases, broad areas of the spectra were fit to sixth degree polynomials (using data points only in areas where no absorption features were observed) to reduce remaining curved backgrounds.

Atomic Force Microscopy. Atomic force microscopy (AFM) experiments were performed in contact mode using a Multimode Nanoscope IV instrument. Measurements of the molecular layer thickness were performed at higher sample-tip forces to scratch away the molecular layer in a square 1 × 1 μm region followed by imaging a larger 4 × 4 μm region centered at the same spot. Experiments were conducted using a range of forces to determine conditions under which the molecular layers could be reliably removed without scratching the underlying TiO_2 surface. Diamond-like carbon (DLC)-coated Si AFM tapping probes (Tap300DLC, Budget Sensors) with a force constant of 40 N/m were used to perform the surface scratching and imaging.

Nuclear Magnetic Resonance (NMR). ^{1}H NMR spectra were obtained using a Varian Mercury-Plus 300 (300 MHz) instrument using $CDCl_3$ as the solvent. Chemical shifts (δ) are reported in parts per million (ppm) with the $CDCl_3$ reference peak set to 7.24 ppm for all spectra. Hexamethylbenzene was added to some samples as an internal standard for quantification.

Mass Spectrometry. Mass spectrometry was performed on NMR samples to confirm NMR findings. A Waters (Micromass) AutoSpec was used to collect spectra, using electron impact ionization with 70 eV electrons. Perfluorokerosene was used to calibrate the AutoSpec.

RESULTS

Reaction of Aryl Halide with TiO_2 Surfaces. As depicted in Figure 1, we investigated aryl compounds of the form 4-halo-1-(trifluoromethyl)benzene, which we refer to as "iodo-TFMB", "bromo-TFMB", and "chloro-TFMB", along with the 4-methyl-1-(trifluoromethyl)benzene (methyl-TFMB). The trifluoro compounds were chosen because the $-CF_3$ group serves as a good marker in XPS and is itself unreactive toward TiO_2 (vide infra).[39] Figure 2 shows XPS data for the F(1s) region for all three aryl halides and methyl-TFMB, which we use as a control sample. XPS data are also shown for the I($3d_{5/2}$), Br(3d), and Cl(2p) regions for the halogenated compounds and for methyl-TFMB. Spectra of the Ti(2p), O(1s), and C(1s), regions are shown in the Supporting Information. In Figure 2, the F(1s) spectrum of the sample exposed to iodo-TFMB shows a single, sharp F(1s) feature at 689.4 eV. The sample exposed to bromo-TFMB also shows some F(1s) intensity near at 689.2 eV, but it is significantly smaller than that observed for the sample exposed to iodo-TFMB, while TiO_2 samples exposed to chloro-TFMB or to methyl-TFMB show no significant F(1s) intensity. The I($3d_{5/2}$) spectrum from iodo-TFMB shows only a very small peak, while the Cl(2p) spectrum from chloro-TFMB and the Br(3d) spectrum from bromo-TFMB show no detectable intensity above the noise level. Samples exposed to methyl-

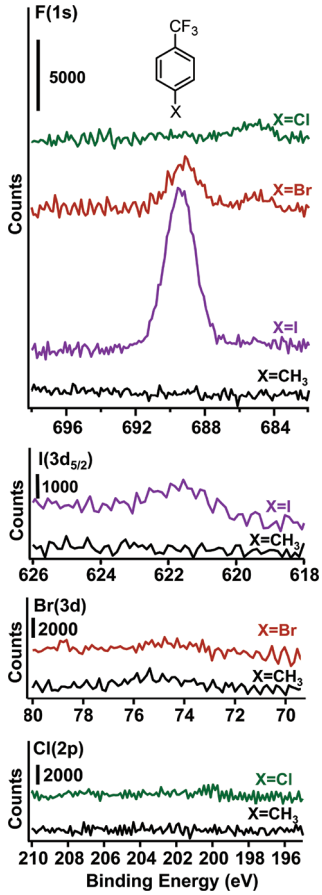

Figure 2. F(1s) XPS data from nanocrystalline TiO_2 films after reaction with aryl halide compounds for 12 h at 50 °C. The bottom trace shows data for methyl-TFMB as a control having a nonreactive group bound to the aromatic ring in place of a halogen.

TFMB show no F, Cl, Br, or I signal. The trend in reactivity observed in the F(1s) spectrum is also reflected in the C(1s) spectra shown in the Supporting Information, although interpretation of C(1s) spectra is complicated by small amounts of contamination that is unavoidable in benchtop chemistry; thus, the F(1s) intensity from the CF_3 group serves as a more robust measure of the extent of adsorption. The Ti(2p) and O(1s) spectra are nearly identical for all four samples; these spectra reflect primarily the underlying substrate and can be used as an internal standard for quantitative analysis.

The data show that iodo-TFMB and, to a lesser extent, bromo-TFMB react with the TiO_2 surface under the relatively mild conditions used here, while chloro-TFMB and methyl-TFMB show no detectable reaction. Quantitative analysis of the XPS data using the Ti(2p) peak as an internal standard yield molecular coverages of 0.8 ± 0.2 molecules/nm^2 for bromo-TFMB, and 2.0 ± 0.1 molecules/nm^2 for iodo-TFMB. This is slightly lower than the values obtained for densely packed phenyl rings on Si(111) surfaces,[40] but still reflects a comparatively dense layer. Analysis of the Br(3d) and I(3d) regions shows that bromo-TFMB leaves no detectable bromine on the surface and iodo-TFMB shows only a trace amount of iodine, with quantitative analysis yielding a coverage of 0.17 iodine atoms/nm^2. On the basis of the I:F ratio (after correction for relative sensitivity factors and the I:F ratio of 1:3 for iodo-TFMB), this corresponds to approximately 0.1 iodine atom on the surface per iodo-TFMB molecule adsorbed

dx.doi.org/10.1021/la300271h | Langmuir 2012, 28, 6866−6876

onto the surface. The absence of any detectable F(1s) intensity after exposure to methyl- or chloro-TFMB shows that the binding of iodo-TFMB and bromo-TFMB is a direct result of the presence of the Br or I groups and does not arise from the aromatic ring or the $-CF_3$ group. However, the low concentration of Br and I atoms on the surface demonstrates that adsorption of iodo-TFMB and bromo-TFMB onto the surface involves breaking C–I or C–Br bonds, and that the halogen byproducts of the reaction are rinsed away.

These results are consistent with what would be expected from the reaction depicted in Figure 1a, in which the incoming molecules interact with surface Ti–OH groups to form Ti–O–C bonds and eliminate HBr or HI. Despite the apparent simplicity of this reaction on paper, it is well-known in organic chemistry[32] that aryl halides like those used here typically show very little reactivity toward alcohols in the absence of a catalyst due to both the steric and the electronic effects that greatly inhibit the most common nucleophilic substitution (S_N2) reaction pathway. For example, previous studies of aryl bromides and iodides showed almost no reaction with liquid-phase *tert*-butanol in the absence of a catalyst.[34,36]

Comparison with Benzyl Halides. To understand how differences in molecular structure impact reactivity on TiO_2 surfaces, we also investigated the bonding of benzyl halides with TiO_2. In this case, the nonaromatic nature of the pendant CH_2X group (where X = Cl, Br, I) is expected to yield reactivity more like that of the classical Williamson ether synthesis. Figure 3 shows F(1s) XPS data for nanocrystalline TiO_2 films that

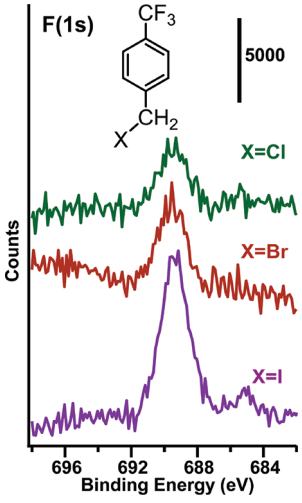

Figure 3. F(1s) XPS data for nanocrystalline TiO_2 films after reaction with benzyl halide compounds for 12 h at 50 °C (X = Cl, Br, H). Because of its higher melting point, a temperature of 80 °C was used for 4-iodomethyl-TFMB (X = I).

were exposed to 4-(halomethyl)-1-(trifluoromethyl)benzene derivatives (which we refer to as "chloromethyl-TFMB," "bromomethyl-TFMB", and "iodomethyl-TFMB"). XPS data for the Ti(2p), O(1s), C(1s), Cl(2p), Br(3d), and I(3d) regions are shown in the Supporting Information. In Figure 3, all three halides show some F(1s) intensity at 689.5 eV, with the iodomethyl-TFMB clearly showing the highest intensity. Using the Ti(2p) peaks as an internal standard for quantitative analysis yields molecular coverages of 1.1 molecules/nm^2 for iodomethyl-TFMB, as compared to only 0.37 molecules/nm^2 for chloromethyl-TFMB, and 0.31 molecules/nm^2 for bromomethyl-TFMB. As with the aryl halides, the absence of detectable intensity from the displaced halogen atoms indicates that molecular adsorption is accompanied by C–X bond cleavage, with the HX byproducts rinsed away from the surface. The maximum surface coverage obtained for iodomethyl-TFMB is slightly smaller than that observed with iodo-TFMB (shown in Figure 2). This suggests that the additional CH_2 group may introduce additional steric interactions that limit the molecular density. While a direct comparison of reactivity is complicated by the fact that the iodomethyl-TFMB experiments were performed at a higher temperature (80 °C) as compared to the other compounds investigated (50 °C for all others), the higher surface coverage of iodomethyl-TFMB as compared to bromomethyl-TFMB or chloromethyl-TFMB is consistent with the reactivity trend (I > Br > Cl > F) typically found with the Williamson ether synthesis.

Comparison of Base- versus Acid-Treated Samples toward Aryl Iodide. The most likely structure for binding aryl and benzyl halides to the TiO_2 surface is via the surface hydroxyl group, releasing HX and forming a Ti–O–C bond at the interface as depicted in Figure 1. To facilitate understanding of this reaction, we investigated whether manipulating the concentration of surface hydroxyl groups and/or their protonation state affected the grafting of the aryl iodide to TiO_2 surfaces. Because the isoelectric point of TiO_2 in water is approximately 5.9,[41] treatment with base is expected to increase the concentration of deprotonated Ti–O$^-$ groups, while the acidic piranha solution is expected to yield protonated Ti–OH groups. To this end, we compared grafting on samples immersed in the piranha solution with grafting on samples treated with NaOH solution using procedures described in the Experimental Section. Figure 4 compares the C(1s) and F(1s) data from piranha-treated and base-treated TiO_2 samples, showing spectra both before and after exposure to iodo-TFMB (50 °C, 24 h). Similar data are shown for the Ti(2p), O(1s), and I(3d) peaks in the Supporting Information. The F(1s) data

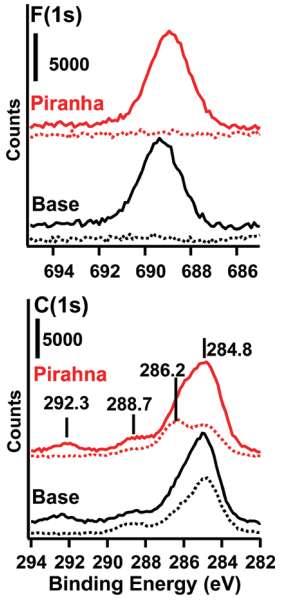

Figure 4. F(1s) and C(1s) XPS data from nanocrystalline TiO_2 samples prepared using piranha treatment and base treatment. Data are shown on freshly treated samples before (- - - -) and after (—) exposure to iodo-TFMB.

dx.doi.org/10.1021/la300271h | *Langmuir* 2012, 28, 6866–6876

show no fluorine on either sample before grafting of iodo-TFMB, which after grafting both show F(1s) peaks with very similar widths and intensities. The C(1s) spectra (Figure 4b) show that before grafting the base- and piranha-treated samples both show some initial carbon contamination, with three peaks that are usually attributed to alkane-like C (284.8 eV), C−OH groups (286.2), and C═O groups (288.7 eV).[42] The total amount of carbon contamination is similar for both samples, although the piranha-treated sample shows a higher proportion of carbon at ∼286.2 eV (alcohol-like) and a lower amount at 284.8 eV (alkane-like), consistent with the highly oxidizing properties of piranha solution. After grafting of iodo-TFMB, both samples show significant increases in C(1s) intensity. Notably, both C(1s) spectra show a new feature at a high binding energy of 292.3 eV, which is similar in energy to that reported previously from $-CF_3$ groups.[43,44] This peak further confirms the successful grafting of iodo-TFMB to the surface. The Ti(2p) and O(1s) spectra in the Supporting Information show no significant differences among the samples, reflecting primarily the bulk Ti and O. By measuring the area of the F(1s) and Ti(2p) peaks, we determined that both piranha and base treatments produced equivalent molecular densities of 1.9 molecules/nm^2. Measurement of the I($3d_{5/2}$) spectra showed that the density of iodine atoms on the surface is <0.3 atoms/nm^2. This density is much less than the density of grafted molecules on the surface, thereby showing that the grafting of the molecules is accompanied by release of iodine atoms into the liquid-phase reactant mixture.

To gain further insights into how the surface hydroxyl composition impacts the grafting, we used FTIR spectroscopy to characterize the samples. Figure 5a and b shows FTIR spectra of the O−H stretching region of piranha-treated (Figure 5a) and base-treated (Figure 5b) samples before and after exposure to iodo-TFMB at 50 °C for 24 h, using a planar, oxidized Ti film as the reference sample. Comparing the "before grafting" spectra of the piranha (Figure 5a) and base-treated (Figure 5b) samples shows that these two treatments yield significantly different distributions of −OH groups: the piranha treatment leads to a broad peak centered near 3660−3665 cm^{-1}, while the base treatment leads to several well-defined peaks at 3632, 3664, and 3695 cm^{-1}, with an overall intensity that is several times higher than that of the piranha-treated sample (note the difference in vertical scales). These spectra are very similar to those published previously.[45] While interpretation is complicated due to overlapping peaks from surface −OH groups and adsorbed water, these previous studies have attributed features at 3730 cm^{-1} to terminal −OH groups, and peaks near 3670 cm^{-1} to bridging −OH groups. Broader features in the 3630−3690 cm^{-1} region are attributed to adsorbed water molecules.[46] Figure 5c shows the difference spectra (after grafting − before grafting), reflecting the change in IR absorbance induced by the 50 °C grafting reaction on the piranha- and base-treated nanocrystalline samples; also shown in this figure are results from a similar experiment performed using (trifluoromethyl)benzene (TFMB), which lacks a halide group on the aromatic ring. The piranha-treated and base-treated samples both show significant decreases in −OH intensity after grafting. Surprisingly, we also observe a similar decrease in −OH intensity on samples that have been exposed to (trifluoromethyl)benzene. We have established separately that TFMB, like methyl-TFMB (see Figure 2), does not bind to TiO_2 to any detectable extent under the conditions used here. In addition to the 50 °C data presented here, experiments using

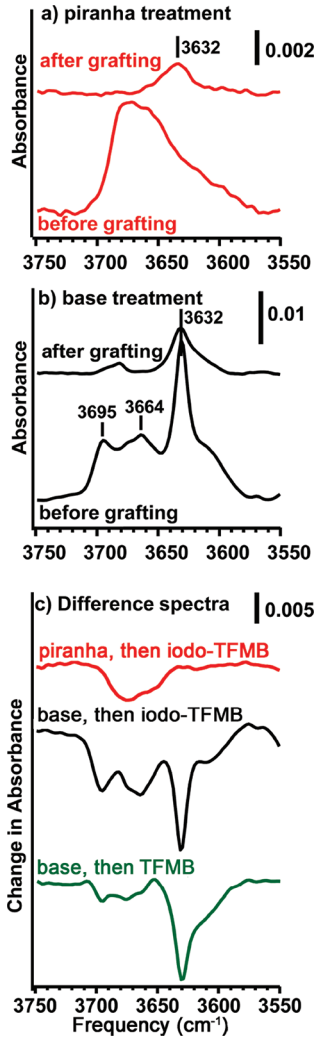

Figure 5. Infrared spectra of TiO_2 samples with different pretreatments and influence on grafting of iodo-TFMB. (a) Spectra of piranha-treated sample before and after grafting; (b) spectra of base-treated sample before and after grafting; and (c) change in absorbance due to grafting of iodo-TFMB on piranha- and base-treated samples, and comparison with similar results for TFMB.

TFMB were also performed at 80 °C for 24 h; the resulting spectra, reported in the Supported Information, showed that heating in TFMB at 80 °C induced a slightly greater loss of hydroxyls as compared to the results obtained at 50 °C, but otherwise there were no significant differences in behavior.

These experiments demonstrate that while grafting of the iodo-TFMB to the surface is accompanied by loss of −OH groups under the reaction conditions used, a similar loss of −OH groups is also observed with a nonreactive compound (i.e., TFMB). Consequently, while heating in iodo-TFMB induces a loss of surface hydroxyl groups, the FTIR data cannot provide a direct link between formation of new surface bonds and the loss of −OH groups. In replicate tests on multiple samples, XPS measurements showed that the base treatment resulted in slightly more consistent values of the molecular density. Because of this greater reproducibility and because handling of the base is less hazardous than working with piranha solution, all further experiments described below were performed using base-treated samples only.

dx.doi.org/10.1021/la300271h | *Langmuir* 2012, 28, 6866−6876

Grafting Time and Surface Coverage. To determine the optimal duration of the grafting reaction and to determine whether the surface reactions are self-terminating (forming a layer with defined thickness, followed by no further reaction), we used FTIR to characterize the time-dependent changes in vibrational spectra and used XPS to characterize the intensity of the F(1s) peak on base-treated samples exposed to iodo-TFMB at 50 °C for different lengths of time. Figure 6 shows FTIR

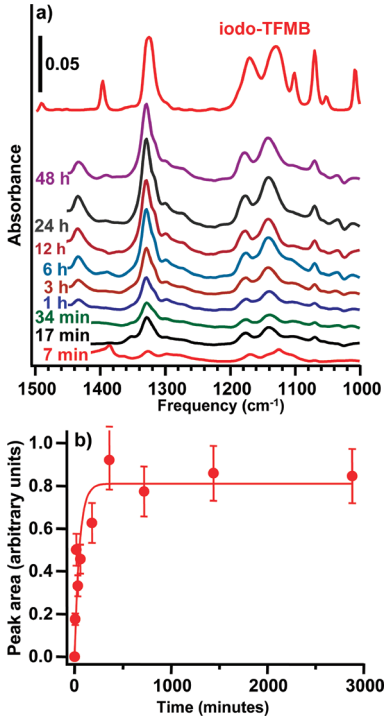

Figure 6. (a) FTIR spectra of base-treated TiO_2 samples after exposure to iodo-TFMB at 50 °C for different lengths of time; and (b) area of 1143 cm^{-1} peak versus time and fit to single-exponential increase.

spectra of a thin film of liquid iodo-TFMB (measured in transmission) and of the base-treated samples after reaction (measured using single-bounce external reflection). Figure 6b shows a graph of the area $A(t)$ of the 1143 cm^{-1} trifluoromethyl peak versus time along with a fit to a simple exponential growth $A(t) = A_0(1 - e^{-t/\tau})$, where A_0 is the maximum absorbance and τ is the time constant for grafting; this fit yielded a time constant τ = 51 min. Similar times were also obtained using other characteristic vibrational modes. XPS data also confirm that the reaction is nearly complete within ~3 h; however, to ensure the maximum possible coverage, we typically allowed the reactions to proceed for 24 h. The Supporting Information shows F(1s), C(1s), I(3d), Ti(2p), and O(1s) data from a nanocrystalline sample that was reacted for 24 h. Repeated measurements show that at the longest grafting times of ~24 h, the F(1s) data show a limiting coverage of 2.0 molecules/nm^2. The surface iodine coverage after 24 h grafting time is ~0.3 atoms/nm^2, similar to the values reported above after ~12 h grafting times. In both cases, there is much less than 1 iodine atom remaining on the surface per molecule adsorbed molecule.

Thickness and Uniformity of Molecular Layer on TiO_2 Surface. Further insights into the nature of the grafting reaction were obtained from atomic force microscopy experiments. These experiments used single-crystal rutile TiO_2 (110) samples to achieve the requisite surface flatness. While rutile and anatase have different crystal structures, previous studies of TiO_2 have shown that the reactions both are controlled largely by local atomic geometry of the titanium and oxygen sites, which are similar on the crystal surfaces.[47−49] Reactants with only a single binding group are also expected to be less sensitive to the detailed geometry than bidentate ligands commonly investigated. Figure 7 shows atomic force microscopy images of a TiO_2 (110) sample that was treated with base as described above. This sample shows very flat, uniform terraces separated by multiple-height steps. Figure 7b shows an image after a base-treated sample was exposed to iodo-TFMB for 24 h at 50 °C. The sample shows a very uniform surface, with small steps

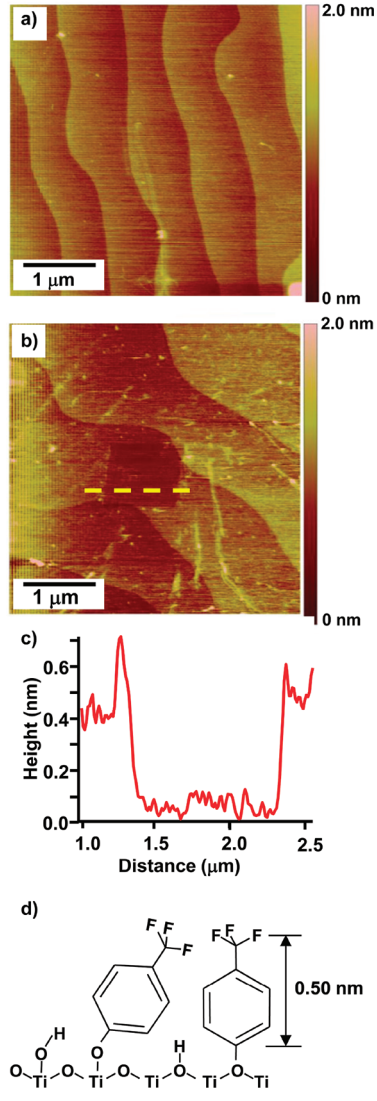

Figure 7. Atomic force microscope images of rutile TiO_2 (110) samples before and after grafting of iodo-TFMB to the surface. (a) Image of TiO_2 sample after cleaning in base, but not exposed to iodo-TFMB. (b) Image of sample grafted with iodo-TFMB and used in an AFM "nano-shaving" experiment as described in text. (c) AFM height profile showing the change in height across the square region scratched away; the regions at left and right correspond to the full molecular layer. (d) Possible molecular structures on surface, and dimensions based on molecular mechanics model.

dx.doi.org/10.1021/la300271h | *Langmuir* 2012, 28, 6866−6876

readily visible on the surface. Within the individual terraces, the surface structure appears very uniform, with almost no surface irregularities. This demonstrates that the grafting process leads to a highly uniform molecular layer.

To verify that the molecular grafted layers are 1 molecule thick, we used the AFM tip to remove the molecular layer from a square 1 μm × 1 μm region (a process sometimes referred to as "nanoshaving"[50]) and then imaged a larger (4 μm × 4 μm) region centered at approximately the same location. The molecular layers were removed by operating the AFM in contact mode using a force strong enough to scratch away a molecular layer (if present) but not strong enough to scratch the underlying TiO_2, as determined by testing different scratching forces on a bare control sample. Figure 7b shows an AFM image of a TiO_2 (110) surface that was functionalized with iodo-TFMB (50 °C, 24 h) and then subjected to the nanoshaving experiment. The region where the molecular layer was removed appears as a small but distinct square region that is 0.45 ± 0.10 nm lower than the surrounding molecular layer. Figure 7d shows the two most likely configurations for the molecular layer, along with surface hydroxyl groups. Using a simple molecular mechanics model with typical bond lengths,[51] we estimate that the molecule is 0.50 nm from the plane of the F atoms to the last aromatic C atom that links to the surface. While molecules may also tilt, these changes in height associated with modest tilts are not expected to be more than ~0.1 nm. Thus, the AFM data definitively show that the grafting reaction leads to a highly uniform molecular monolayer.

Comparison of Surface Grafting Reactions with Liquid-Phase Reactions. The above experiments demonstrate that aryl iodide compounds such as iodo-TFMB react with the TiO_2 surface to yield molecular layers that are covalently bonded to the surface. To compare the behavior of surface Ti−OH groups with the C−OH more typically encountered in synthetic chemistry, we evaluated the reactivity of the iodo-TFMB and iodomethyl-TFMB with *tert*-butanol, both with and without added *tert*-butoxide. The products were characterized using NMR and mass spectrometry. The NMR spectra are shown in the Supporting Information, with the results summarized in Figure 8. For clarity, we have numbered the reactants and likely products in Figure 8. In the first set of experiments, depicted in Figure 8a and b, we made equimolar mixtures of the halide reactant (either **1** or **4**) with *tert*-butanol (**2**) and heated the mixtures for 12 h at 80 °C for the benzyl compound (**4**) and 50 °C for the aryl compound (**1**), thereby simulating conditions used in the surface experiments. A comparison of the NMR spectra before and after reaction (shown in the Supporting Information) showed no evidence for NMR signatures associated with the products **3** and **5**, and appeared essentially identical to those of the starting materials. On the basis of these experiments, we concluded that neither the aryl iodide (**1**) nor the benzyl iodide (**4**) reacts with *tert*-butanol (**2**). Because the Williamson ether synthesis is typically performed under basic conditions, we also performed experiments in which sodium *tert*-butoxide salt (**6**) was added. When starting with iodo-TFMB (**1**), the NMR spectra showed no evidence for formation of the anticipated product (**3**). However, when using iodomethyl-TFMB (**4**), NMR showed facile conversion to the reaction product (**5**).

These NMR experiments show that when coupled with a simple organic alcohol, the aryl and benzyl iodides behave in the manner commonly reported for the Williamson ether synthesis. Specifically, under the conditions used in these experiments, the aryl compound iodo-TFMB does not react with simple alcohols or alkoxides, while the benzyl compound iodomethyl-TFMB reacts with alkoxides but not alcohols. The fact that we observe iodo-TFMB reacting with the TiO_2 surface indicates that the reactivity of iodo-TFMB is distinct from that of typical organic reaction and is not a simple consequence of the presence of surface hydroxyl groups.

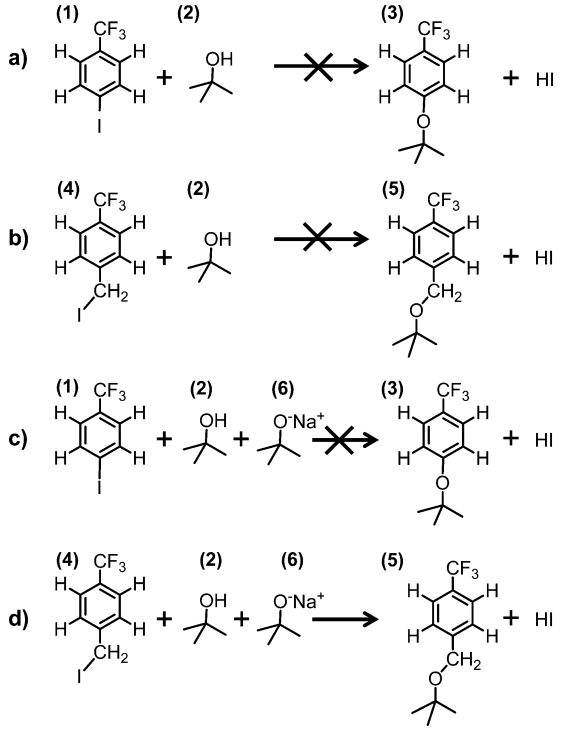

Figure 8. Summary of possible reactions of iodo-TFMB (a,c) and iodomethyl-TFMB (b,d) with *tert*-butanol and *tert*-butanol/sodium *tert*-butoxide mixtures. NMR data show that only reaction (d) occurs to any detectable extent.

Molecular Layer Stability. To test the stability of the organic layers in water, we conducted experiments in which base-treated TiO_2 samples were functionalized with iodo-TFMB. The freshly functionalized samples were then immersed in 50 °C nanopure water and removed for analysis via FTIR after different time intervals. The sum of the area of five FTIR peaks at 1329, 1316, 1178, 1143, and 1069 cm^{-1} were used to evaluate the coverage. Figure 9 shows the change in total area for these five peaks over a period of 6 h, along with a fit to a simple exponential $A(t) = A_0 \exp^{-t/t_{des}}$, where A_0 is the absorbance at time = 0 min, and t_{des} is the characteristic time constant for desorption. The fit yields a value of t_{des} = 100 ± 20 min.

The stability we observe in aqueous solution is significantly better than that observed with simple monodentate ligands such as carboxylic acids,[8,21,52] but not as good as layers produced by photochemical grafting of alkenes[23] or by thermal grafting of silanes[11,15,16] or phosphonic acids.[11,16] However, the stability of the these latter approaches is likely due at least in part to lateral cross-linking and/or multilayer formation.[11,16,18,22] It is likely that Ti−O−C bonds are susceptible to hydrolysis and that the alkyl chains play an important role in controlling stability by preventing water access to the interfacial bonds.[11] In our case, the improved stability we observe as compared to simple monodentate carboxylic acids suggests

dx.doi.org/10.1021/la300271h | *Langmuir* 2012, 28, 6866−6876

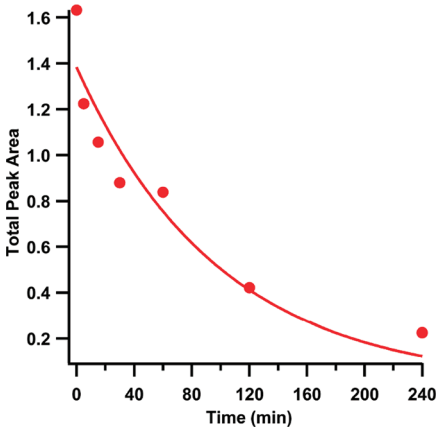

Figure 9. Area of molecular 1329, 1316, 1178, 1143, and 1069 cm^{-1} infrared peaks versus immersion time for TiO_2 sample modified with iodo-TFMB and then immersed in pure water at 50 °C for the indicated times.

formation of layers that are sufficiently dense that they are able to resist water penetration for a limited period of time.

DISCUSSION

Our experiments demonstrate that iodo-TFMB (an aryl iodide) and iodomethyl-TFMB (a benzyl iodide) both react with hydroxylated TiO_2 surfaces under mild thermal conditions to form dense molecular monolayers. The reaction of the aryl iodide is particularly surprising and potentially important because it may provide a route to directly link more complex conjugated π-electron systems such as organic dyes or catalysts based on coordination complexes to TiO_2 surfaces, with no additional pendant atoms or functional groups between the aromatic ring and the surface. In the case of benzyl halides, the grafting yields conjugated molecules linked to the surface via a single-atom linker. In both cases, the ability to achieve such short molecular tethers may be expected to lead to high electron-transfer rates relevant to fields such as solar energy conversion using dye-sensitized solar cells.[9,37,38] Studies of electron transfer in dye-sensitized solar cells have shown that the ultrafast transfer of photoexcited electrons from the molecule to the TiO_2 depends on the degree of electron delocalization between the π-conjugated electrons of the molecule and the conduction band of the TiO_2.[38,53−55] In contrast to the work presented here, the vast majority of studies use carboxylate linkages that involve at least one carbon atom between aromatic rings and the TiO_2.[2−5,9,37,56] The most common of these involves pendant carboxylate linkages that bind to the surface Ti ions via a 2-atom bridge. Our results provide an alternative mode of binding with the aromatic ring directly bonded to surface oxygen sites.

The high reactivity of aryl iodides (and, to a lesser extent, aryl bromides) is somewhat unexpected. In a previous study,[29] we reported that simple alkyl iodides reacted with TiO_2 to form well-defined monolayers and that, due to the ubiquitous Ti−OH groups present under ambient conditions,[48] this reaction appeared analogous to the well-known Williamson ether synthesis of organic chemistry.[31] The Williamson ether synthesis is generally described as a bimolecular nucleophilic substitution (S_N2) reaction in which a deprotonated alcohol attacks the antibonding σ^* orbital of a carbon−halogen bond, expelling the halide ion and forming an ether linkage as depicted in Figure 1.[32,36,57] Such S_N2 reactions typically are facile with benzyl and alkyl halides but generally do not proceed to any appreciable extent with aryl halides due to steric and electronic constraints imposed by the benzene ring.[32−34] Etherification reactions with aryl halides are known, but typically proceed by the much less facile nucleophilic aromatic substitution, benzyne, or radical reaction mechanisms.[58] For example, Cadogan et al.[36] showed that bromo-TFMB and other aryl bromides slowly react with potassium *tert*-butoxide via loss of HBr, forming aryne intermediates that are subsequently attacked by a nucleophile, yielding ether products. However, the conditions of this experiment were quite harsh (>150 °C for >4 h) as compared to the conditions used in our experiments. Prior studies of aromatic nucleophilic substitution ("S_NAr") reactions of halogen-modified aromatics have typically observed that the different halogens yield a reactivity trend that is the *opposite* of that we observe.[59]

Elucidation of a detailed mechanism for the surface reaction is complicated by the presence of multiple crystal faces and the many overlapping features due to surface −OH groups and modes of adsorbed water. Prior studies of TiO_2 surfaces have revealed spectra much like those depicted in Figure 5a and b, with the spectra varying considerably depending on the past history of the TiO_2 and subsequent treatments.[45] In those studies, samples showing a preponderance of −OH modes near 3630 cm^{-1} were found to have nucleophilic character toward benzaldehyde (thereby acting as Lewis bases), while samples with a preponderance of peaks near 3665 cm^{-1} were found to have more Lewis acid character.[45] Our FTIR experiments show that acid- versus base-treatment indeed shifts the distribution of −OH species, but this shift does not appear to have a substantial effect on the thermal grafting of iodo-TFMB.

Our experiments demonstrating that iodo-TFMB grafts to TiO_2 but does not readily react with *tert*-butanol or sodium *tert*-butoxide demonstrate that the TiO_2 surface has reactivity greater than that expected from the exposed −OH groups alone. We believe a key to this reactivity lies in the fact that TiO_2 surfaces are only partially hydroxylated. For example, the bulk-truncated anatase(001) surface (the lowest-energy face) exposes 7.0 under-coordinated Ti atoms/nm^2 and an equal number of under-coordinated oxygen atoms; a fully hydrated anatase(001) surface would therefore yield 14 hydroxyl groups/nm^2. Because experimental measurements show lower values of ~3−4 hydroxyl groups/nm^2,[26,27] this indicates that only ~25% of the surface sites are associated with hydroxyl groups and the remaining sites remain uncoordinated. Consequently, an impinging reactant such as iodo-TFMB would likely interact with both hydroxylated and nonhydroxylated surface sites. One possibility is for the iodo-TFMB to interact both with an under-coordinated Ti site (a Lewis acid site) and with a deprotonated hydroxyl group (a Lewis base site), as depicted in Figure 10.

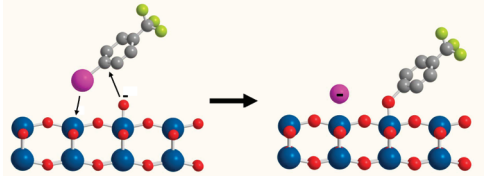

Figure 10. Schematic depicting possible interaction of iodo-TFMB with anatase(001) surface, showing surface Ti ion interacting with iodine and surface O^- (deprotonated hydroxyl) interacting with aryl C atom. Ti atoms are shown in blue, O atoms in red, C atoms in gray, F in yellow, and I in purple.

dx.doi.org/10.1021/la300271h | *Langmuir* 2012, 28, 6866−6876

Here, the interaction of the terminal iodine of iodo-TFMB with a bare Ti^{4+} site would be expected to weaken the C−I bond, enhancing the ability of an adjacent (deprotonated) hydroxyl group to initiate nucleophilic attack on the aryl C atoms, inducing C−I bond cleavage. This general idea was proposed earlier to explain the formation of phenoxide groups when TiO_2 that was exposed to iodobenzene in vacuum was heated to 150 °C;[60] our results indicate that this or a similar pathway likely plays an important role in enabling monolayer formation from aryl iodides on TiO_2 under the near-ambient conditions explored here.

The overall density of grafted molecules (2.0 molecules/nm^2 for iodo-TFMB and 1.1 molecules/nm^2 for iodomethyl-TFMB) is smaller than the number of hydroxyl groups and is likely limited by steric interactions. Prior studies have reported that benzenethiol monolayers on gold can reach ∼4 molecules/nm^2,[61] and similar values have been reported on Si(111) via diazonium chemistry;[40] however, in the latter case, the surface bonding configuration forces the aromatic bonds to be exactly perpendicular to the surface, facilitating dense-packing. Our molecules are slightly larger due to the terminal CF_3 group and, for iodomethyl-TFMB, the additional methylene spacer. Further studies will be necessary to fully elucidate how the grafting density depends on the specific types of surface groups accessible. Notably, however, the surface densities we measure here are still larger than the surface densities of dye molecules commonly used in dye-sensitized solar cells, which are typically ∼0.5−1.5 molecule/nm^2.[62,63]

Unlike the prior work on vacuum-dosed surfaces,[30,60] our results demonstrate that only modest temperatures of ∼50−80 °C are needed to induce the reaction of aryl and benzyl iodides with TiO_2. However, we still observed that the reaction is activated and that at room temperature grafting of the iodo compounds is very slow. Activation could be associated with the actual displacement reaction like that depicted in Figure 10, or possibly by penetration of the reactant molecules through the layer of tightly bound water molecules that are hydrogen-bonded to the surface −OH groups. A previous study of the adsorption of gas-phase chlorobenzene on TiO_2 in air of varying humidity levels found that adsorption was limited by the penetration of the molecules through the adsorbed water layer, rather than subsequent interaction with the surface.[64] Our FTIR experiments show that under the conditions of successful grafting, both reactive (e.g., iodo-TFMB and iodomethyl-TFMB) and nonreactive (e.g., methyl-TFMB) molecules displace water from the near-surface region; this is demonstrated by the removal of nearly all of the −OH stretching vibrations (see Figure 4) after heating to 50 °C. While this suggests that displacement of surface water may be the rate-limiting step, we also note that we observe large differences in reactivity between the iodo-, chloro-, and bromo-compounds. Because all molecules investigated here would be expected to penetrate the surface water with similar efficacy, this indicates that the lack of reactivity of the chloro and bromo compounds under the conditions of our experiments is not associated with inability to penetrate to the surface, but is associated with the intrinsically higher bond strength and reduced reactivity of these compounds as compared to the iodo compound. Further studies will be needed to identify the rate-limiting steps for reaction of the iodo compound.

While a detailed mechanism of the grafting of aryl halides onto TiO_2 remains elusive, the practical utility of the reaction is significant as it provides a new route to linking π-conjugated electron systems to TiO_2 surfaces. The short, direct linkage from the conjugated electron system to the surface may facilitate ultrafast electron transfer. In addition, the aqueous stability of the grafted layers appears better than the stability of simple carboxylate linkages, suggesting that monolayers grafted as described herein may provide increased stability against hydrolysis.

■ CONCLUSION

The above results demonstrate a new approach to grafting π-conjugated electron systems to titanium dioxide with the shortest possible molecule-surface tether. The use of aryl iodides (and possibly bromides) provides rapid reaction and results in dense, highly uniform and homogeneous π-conjugated molecular layers. While the reaction of alkyl and benzyl iodides with −OH groups has clear precedence in the well-known Williamson ether synthesis of organic chemistry, similar reactions with aryl iodides are widely regarded as kinetically unfavorable in the absence of a catalyst. Our results show that TiO_2 surfaces are able to catalyze the reaction, allowing formation of well-defined molecular layers of π-conjugated molecules using benchtop chemistry.

■ ASSOCIATED CONTENT

Supporting Information

Synthesis of 1-(iodomethyl)-4-(trifluoromethyl)benzene. Method of calculating surface coverages. Additional XPS data for aryl and benzyl compounds. FTIR data comparing loss of −OH intensity at 80 and 50 °C. XPS data for iodo-TFMB after 24 h reaction time. NMR spectra characterizing interaction of iodo-TFMB and iodomethyl-TFMB with *tert*-butanol and sodium *tert*-butoxide, with peak assignments. This material is available free of charge via the Internet at http://pubs.acs.org.

■ AUTHOR INFORMATION

Corresponding Author

*E-mail: rjhamers@wisc.edu.

Notes

The authors declare no competing financial interest.

■ ACKNOWLEDGMENTS

This work was supported by the National Science Foundation grant CHE0911543. Dr. Martha M. Vestling is acknowledged for recording mass spectral data.

■ REFERENCES

(1) Hugenschmidt, M. B.; Gamble, L.; Campbell, C. T. The interaction of H_2O with a TiO_2(110) surface. *Surf. Sci.* **1994**, *302*, 329−340.

(2) Oregan, B.; Gratzel, M. A low-cost, high-efficiency solar-cell based on dye-sensitized colloidal TiO_2 films. *Nature* **1991**, *353*, 737−740.

(3) Kroeze, J. E.; Hirata, N.; Koops, S.; Nazeeruddin, M. K.; Schmidt-Mende, L.; Gratzel, M.; Durrant, J. R. Alkyl chain barriers for kinetic optimization in dye-sensitized solar cells. *J. Am. Chem. Soc.* **2006**, *128*, 16376−16383.

(4) Hagberg, D. P.; Yum, J. H.; Lee, H.; De Angelis, F.; Marinado, T.; Karlsson, K. M.; Humphry-Baker, R.; Sun, L. C.; Hagfeldt, A.; Gratzel, M.; Nazeeruddin, M. K. Molecular engineering of organic sensitizers for dye-sensitized solar cell applications. *J. Am. Chem. Soc.* **2008**, *130*, 6259−6266.

(5) Galoppini, E.; Guo, W. Z.; Zhang, W.; Hoertz, P. G.; Qu, P.; Meyer, G. J. Long-range electron transfer across molecule-nanocrystal-

line semiconductor interfaces using tripodal sensitizers. *J. Am. Chem. Soc.* **2002**, *124*, 7801−7811.
(6) Galoppini, E. Linkers for anchoring sensitizers to semiconductor nanoparticles. *Coord. Chem. Rev.* **2004**, *248*, 1283−1297.
(7) Nazeeruddin, M. K.; Pechy, P.; Renouard, T.; Zakeeruddin, S. M.; Humphry-Baker, R.; Comte, P.; Liska, P.; Cevey, L.; Costa, E.; Shklover, V.; Spiccia, L.; Deacon, G. B.; Bignozzi, C. A.; Gratzel, M. Engineering of efficient panchromatic sensitizers for nanocrystalline TiO_2-based solar cells. *J. Am. Chem. Soc.* **2001**, *123*, 1613−1624.
(8) Roncaroli, F.; Blesa, M. A. Kinetics of adsorption of carboxylic acids onto titanium dioxide. *Phys. Chem. Chem. Phys.* **2010**, *12*, 9938−9944.
(9) Asbury, J. B.; Hao, E.; Wang, Y. Q.; Ghosh, H. N.; Lian, T. Q. Ultrafast electron transfer dynamics from molecular adsorbates to semiconductor nanocrystalline thin films. *J. Phys. Chem. B* **2001**, *105*, 4545−4557.
(10) Gamble, L.; Henderson, M. A.; Campbell, C. T. Organo-functionalization of TiO_2(110): (3,3,3-trifluoropropyl)-trimethoxysilane adsorption. *J. Phys. Chem. B* **1998**, *102*, 4536−4543.
(11) Marcinko, S.; Fadeev, A. Y. Hydrolytic stability of organic monolayers supported on TiO_2 and ZrO_2. *Langmuir* **2004**, *20*, 2270−2273.
(12) Fadeev, A. Y.; McCarthy, T. J. A new route to covalently attached monolayers: Reaction of hydridosilanes with titanium and other metal surfaces. *J. Am. Chem. Soc.* **1999**, *121*, 12184−12185.
(13) Song, Y. Y.; Hildebrand, H.; Schmuki, P. Optimized monolayer grafting of 3-aminopropyltriethoxysilane onto amorphous, anatase and rutile TiO_2. *Surf. Sci.* **2010**, *604*, 346−353.
(14) Zuo, J.; Torres, E. Comparison of adsorption of mercaptopropyltrimethoxysilane on amphiphilic TiO_2 and hydroxylated SiO_2. *Langmuir* **2010**, *26*, 15161−15168.
(15) Fadeev, A. Y.; Helmy, R.; Marcinko, S. Self-assembled monolayers of organosilicon hydrides supported on titanium, zirconium, and hafnium dioxides. *Langmuir* **2002**, *18*, 7521−7529.
(16) Helmy, R.; Fadeev, A. Y. Self-assembled monolayers supported on TiO_2: Comparison of $C_{18}H_{37}SiX_3$ (X = H, Cl, OCH_3) $C_{18}H_{37}Si(CH_3)_2Cl$, and $C_{18}H_{37}PO(OH)_2$. *Langmuir* **2002**, *18*, 8924−8928.
(17) Gawalt, E. S.; Lu, G.; Bernasek, S. L.; Schwartz, J. Enhanced bonding of alkanephosphonic acids to oxidized titanium using surface-bound alkoxyzirconium complex interfaces. *Langmuir* **1999**, *15*, 8929−8933.
(18) Gouzman, I.; Dubey, M.; Carolus, M. D.; Schwartz, J.; Bernasek, S. L. Monolayer vs. multilayer self-assembled alkylphosphonate films: X-ray photoelectron spectroscopy studies. *Surf. Sci.* **2006**, *600*, 773−781.
(19) Zapol, P.; Curtiss, L. A. Organic molecule adsorption on TiO_2 nanoparticles: A review of computational studies of surface interactions. *J. Comput. Theor. Nanosci.* **2007**, *4*, 222−230.
(20) Pawsey, S.; Yach, K.; Reven, L. Self-assembly of carboxyalkylphosphonic acids on metal oxide powders. *Langmuir* **2002**, *18*, 5205−5212.
(21) Paoprasert, P.; Kandala, S.; Sweat, D. P.; Ruther, R.; Gopalan, P. Versatile grafting chemistry for creation of stable molecular layers on oxides. *J. Mater. Chem.* **2012**, *22*, 1046−1053.
(22) Franking, R.; Hamers, R. J. Ultraviolet-induced grafting of alkenes to TiO_2 surfaces: Controlling multi layer formation. *J. Phys. Chem. C* **2011**, *115*, 17102−17110.
(23) Franking, R. A.; Landis, E. C.; Hamers, R. J. Highly stable molecular layers on nanocrystalline anatase TiO_2 through photochemical grafting. *Langmuir* **2009**, *25*, 10676−10684.
(24) Gamble, L.; Jung, L. S.; Campbell, C. T. Decomposition and protonation of surface ethoxys on TiO_2(110). *Surf. Sci.* **1996**, *348*, 1−16.
(25) Henderson, M. A. Structural sensitivity in the dissociation of water on TiO_2 single-crystal surfaces. *Langmuir* **1996**, *12*, 5093−5098.
(26) Arrouvel, C.; Digne, M.; Breysse, M.; Toulhoat, H.; Raybaud, P. Effects of morphology on surface hydroxyl concentration: a DFT comparison of anatase-TiO_2 and gamma-alumina catalytic supports. *J. Catal.* **2004**, *222*, 152−166.
(27) Sumita, M.; Hu, C. P.; Tateyama, Y. Interface water on TiO_2 anatase (101) and (001) surfaces: First-principles study with TiO_2 slabs dipped in bulk water. *J. Phys. Chem. C* **2010**, *114*, 18529−18537.
(28) Ryan, M. A.; Spitler, M. T. Light-initiated surface modification of oxide semiconductors with organic dyes. *Langmuir* **1988**, *4*, 861−867.
(29) Chen, J.; Franking, R.; Ruther, R. E.; Tan, Y.; He, X.; Hogendoorn, S. R.; Hamers, R. J. Formation of molecular monolayers on TiO_2 surfaces: A surface analogue of the Williamson ether synthesis. *Langmuir* **2011**, *27*, 6879−6889.
(30) Wu, W. C.; Liao, L. F.; Shiu, J. S.; Lin, J. L. FTIR study of interactions of ethyl iodide with powdered TiO_2. *Phys. Chem. Chem. Phys.* **2000**, *2*, 4441−4446.
(31) Williamson, A. Theory of aetherification. *Philos. Mag.* **1850**, *37*, 350−356.
(32) Sundberg, R. J.; Carey, F. A. *Advanced Organic Chemistry*, 4th ed.; Kluwer Academic/Plenum: New York, 2003.
(33) Mann, G.; Hartwig, J. F. Palladium alkoxides: Potential intermediacy in catalytic amination, reductive elimination of ethers, and catalytic etheration. Comments on alcohol elimination from Ir(111). *J. Am. Chem. Soc.* **1996**, *188*, 13109−13110.
(34) Palucki, M.; Wolfe, J. P.; Buchwald, S. L. Synthesis of oxygen heterocycles via a palladium-catalyzed C-O bond-forming reaction. *J. Am. Chem. Soc.* **1996**, *118*, 10333−10334.
(35) Cramer, R.; Coulson, D. R. Nickel-catalyzed displacement reactions of aryl-halides. *J. Org. Chem.* **1975**, *40*, 2267−2273.
(36) Cadogan, J. I. G.; Hall, J. K. A.; Sharp, J. T. The formation of arynes by reaction of potassium t-butoxide with aryl halides. *J. Chem. Soc. C* **1967**, 1860−1862.
(37) Asbury, J. B.; Hao, E. C.; Wang, Y. Q.; Lian, T. Q. Bridge length-dependent ultrafast electron transfer from Re polypyridyl complexes to nanocrystalline TiO_2 thin films studied by femtosecond infrared spectroscopy. *J. Phys. Chem. B* **2000**, *104*, 11957−11964.
(38) Paoprasert, P.; Laaser, J. E.; Xiong, W.; Franking, R. A.; Hamers, R. J.; Zanni, M. T.; Schmidt, J. R.; Gopalan, P. Bridge-dependent interfacial electron transfer from rhenium-bipyridine complexes to TiO_2 nanocrystalline thin films. *J. Phys. Chem. C* **2010**, *114*, 9898−9907.
(39) Walton, R. M.; Liu, H.; Gland, J. L.; Schwank, J. W. Resistance measurements of platinum-titania thin film gas detectors in ultra-high vacuum (UHV) and reactive ion etcher (RIE) systems. *Sens. Actuators, B* **1997**, *41*, 143−151.
(40) Stewart, M. P.; Maya, F.; Kosynkin, D. V.; Dirk, S. M.; Stapleton, J. J.; McGuiness, C. L.; Allara, D. L.; Tour, J. M. Direct covalent grafting of conjugated molecules onto Si, GaAs, and Pd surfaces from aryidiazonium salts. *J. Am. Chem. Soc.* **2004**, *126*, 370−378.
(41) Kosmulski, M. The significance of the difference in the point of zero charge between rutile and anatase. *Adv. Colloid Interface Sci.* **2002**, *99*, 255−264.
(42) Barr, T. L.; Seal, S. Nature of the use of adventitious carbon as a binding-energy standard. *J. Vac. Sci. Technol., A* **1995**, *13*, 1239−1246.
(43) Wang, X.; Colavita, P. E.; Metz, K. M.; Butler, J. E.; Hamers, R. J. Direct photopatterning and SEM imaging of molecular monolayers on diamond surfaces: Mechanistic insights into UV-initiated molecular grafting. *Langmuir* **2007**, *23*, 11623−11630.
(44) Luo, Y.; Bernien, M.; Krüger, A.; Hermanns, C. F.; Miguel, J.; Chang, Y.-M.; Jaekel, S.; Kuch, W.; Haag, R. In situ hydrolysis of imine derivatives on Au(111) for the formation of aromatic mixed self-assembled monolayers: Multitechnique analysis of this tunable surface modification. *Langmuir* **2011**, *28*, 358−366.
(45) Martra, G. Lewis acid and base sites at the surface of microcrystalline TiO_2 anatase: relationships between surface morphology and chemical behaviour. *Appl. Catal., A* **2000**, *200*, 275−285.
(46) Soria, J.; Sanz, J.; Sobrados, I.; Coronado, J. M.; Maira, A. J.; Hernandez-Alonso, M. D.; Fresno, F. FTIR and NMR study of the adsorbed water on nanocrystalline anatase. *J. Phys. Chem. C* **2007**, *111*, 10590−10596.

(47) Diebold, U. The surface science of titanium dioxide. *Surf. Sci. Rep.* **2003**, *48*, 53−229.
(48) Kung, H. H. *Transition Metal Oxides: Surface Chemistry and Catalysis*; Elsevier Science Publishers B.V.: Amsterdam, 1989.
(49) Lusvardi, V. S.; Barteau, M. A.; Farneth, W. E. The effects of bulk titania crystal-structure on the adsorption and reaction of aliphatic-alcohols. *J. Catal.* **1995**, *153*, 41−53.
(50) Liu, G. Y.; Xu, S.; Qian, Y. L. Nanofabrication of self-assembled monolayers using scanning probe lithography. *Acc. Chem. Res.* **2000**, *33*, 457−466.
(51) Allinger, N. L. Conformational analysis. 130. A hydrocarbon force field utilizing V1 and V2 torsional terms. *J. Am. Chem. Soc.* **1977**, *99*, 9127−8234.
(52) Bishop, L. M.; Yeager, J. C.; Chen, X.; Wheeler, J. N.; Torelli, M. D.; Benson, M. C.; Burke, S. D.; Pedersen, J. A.; Hamers, R. J. A citric acid-derived ligand for modular functionalization of metal oxide surfaces via "Click" chemistry. *Langmuir* **2012**, *28*, 1322−1329.
(53) Heimer, T. A.; Heilweil, E. J. Direct time-resolved infrared measurement of electron injection in dye-sensitized titanium dioxide films. *J. Phys. Chem. B* **1997**, *101*, 10990−10993.
(54) Wiberg, J.; Marinado, T.; Hagberg, D. P.; Sun, L. C.; Hagfeldt, A.; Albinsson, B. Effect of anchoring group on electron injection and recombination dynamics in organic dye-sensitized solar cells. *J. Phys. Chem. C* **2009**, *113*, 3881−3886.
(55) Odobel, F.; Suresh, S.; Blart, E.; Nicolas, Y.; Quintard, J. P.; Janvier, P.; Le Questel, J. Y.; Illien, B.; Rondeau, D.; Richomme, P.; Haupl, T.; Wallin, S.; Hammarstrom, L. Synthesis of oligothiophene-bridged bisporphyrins and study of the linkage dependence of the electronic coupling. *Chem.-Eur. J.* **2002**, *8*, 3027−3046.
(56) Durrant, J. R.; Haque, S. A.; Palomares, E. Towards optimization of electron transfer processes in dye sensitised solar cells. *Coord. Chem. Rev.* **2004**, *248*, 1247−1257.
(57) Cristol, S. J.; Bindel, T. H. Photochemcial transformations. 26. Sensitized and unsensitized photoreactions of some benzyl chlorides in tert-butyl alcohol. *J. Org. Chem.* **1980**, *45*, 951−957.
(58) Anslyn, E. V.; Dougherty, D. A. *Modern Physical Organic Chemistry*; University Science Books: Sausalito, CA, 2006.
(59) Knipe, A. C.; McGuinness, S. J.; Watts, W. E. A kinetic-study of the mechanisms of S_NAr reaction sof neutral and cationic metal-complexed halogenoarenes with methoxide ion. *J. Chem. Soc., Perkin Trans. 2* **1981**, 193−200.
(60) Wu, W. C.; Liao, L. F.; Lien, C. F.; Lin, J. L. FTIR study of adsorption, thermal reactions and photochemistry of benzene on powdered TiO_2. *Phys. Chem. Chem. Phys.* **2001**, *3*, 4456−4461.
(61) Sabatani, E.; Cohenboulakia, J.; Bruening, M.; Rubinstein, I. Thioaromatic monolayers on gold - a new family of self-assembling monolayers. *Langmuir* **1993**, *9*, 2974−2981.
(62) Fillinger, A.; Soltz, D.; Parkinson, B. A. Dye sensitization of natural anatase crystals with a ruthenium-based dye. *J. Electrochem. Soc.* **2002**, *149*, A1146−A1156.
(63) Spitler, M. T.; Calvin, M. Electron-transfer at sensitized TiO_2 electrodes. *J. Chem. Phys.* **1977**, *66*, 4294−4305.
(64) Zhang, L. F.; Anderson, W. A.; Sawell, S.; Moralejo, C. Mechanistic analysis on the influence of humidity on photocatalytic decomposition of gas-phase chlorobenzene. *Chemosphere* **2007**, *68*, 546−553.